JACS
JOURNAL OF THE AMERICAN CHEMICAL SOCIETY
Communication
pubs.acs.org/JACS

Confocal Fluorescence Microscopy Studies of a Fluorophore-Labeled Dirhodium Compound: Visualizing Metal–Metal Bonded Molecules in Lung Cancer (A549) Cells

Bruno Peña,[†] Rola Barhoumi,*[,‡] Robert C. Burghardt,[‡] Claudia Turro,[§] and Kim R. Dunbar*[,†]

[†]Department of Chemistry, Texas A&M University, College Station, Texas 77842, United States
[‡]Department of Veterinary Integrative Biosciences, Texas A&M University, College Station, Texas 77843, United States
[§]Department of Chemistry and Biochemistry, The Ohio State University, Columbus, Ohio 43210, United States

Supporting Information

ABSTRACT: The new dirhodium compound $[Rh_2(\mu\text{-}O_2CCH_3)_2(\eta^1\text{-}O_2CCH_3)(phenbodipy)(H_2O)_3][O_2CCH_3]$ (**1**), which incorporates a bodipy fluorescent tag, was prepared and studied by confocal fluorescence microscopy in human lung adenocarcinoma (A549) cells. It was determined that **1** localizes mainly in lysosomes and mitochondria with no apparent nuclear localization in the 1–100 μM range. These results support the conclusion that cellular organelles rather than the nucleus can be targeted by modification of the ligands bound to the Rh_2^{4+} core. This is the first study of a fluorophore-labeled metal–metal bonded compound, work that opens up new venues for the study of intracellular distribution of dinuclear transition metal anticancer complexes.

Complexes based on the Rh_2^{4+} core are the most well-studied metal–metal (M–M) bonded compounds *vis-à-vis* cancer drug research.[1] The first reports concerning the carcinostatic activity of dirhodium compounds appeared a few years after the discovery of the antitumor properties of cisplatin by Barnett Rosenberg,[2] when John Bear reported that dirhodium tetraacetate ($Rh_2(\mu\text{-}O_2CCH_3)_4$, Figure 1) increased the survival time of mice bearing Ehrlich ascites and L1210 tumors.[3,4] Various anticancer dirhodium compounds with different equatorial bridging ligands[5,6] as well as chelating polypyridyl ligands[7,8] have been reported over the years that exhibit antitumor properties comparable to or better than those of cisplatin. A combination of X-ray crystallography, NMR spectroscopy, mass spectrometry, and biological studies performed in our laboratories and others provides strong evidence that dirhodium tetracarboxylate and formamidinate complexes bind covalently to DNA purines, nucleotides, dinucleotides, and single-stranded and double-stranded DNA, suggesting that nuclear DNA is a potential target of dirhodium compounds *in vivo*,[1] possibly mimicking the mechanism of action of cisplatin.[9]

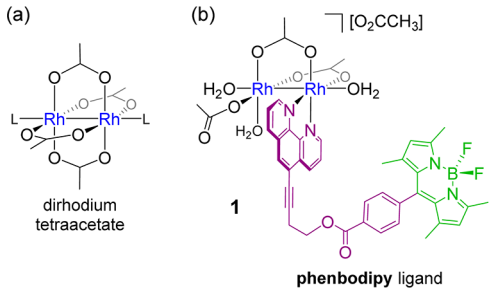

Figure 1. Molecular structures of (a) $Rh_2(\mu\text{-}O_2CCH_3)_4$ and (b) compound **1**. L denotes a coordinated axial solvent molecule.

In 2009, our group reported that compounds of general formula $[Rh_2(\mu\text{-}O_2CCH_3)_2(\eta^1\text{-}O_2CCH_3)(N\text{^}N)(CH_3OH)_3]^+$ (N^N is a polypyridyl ligand) are active against COLO-316 and HeLa cancer cells.[10] The most active complex, $[Rh_2(\mu\text{-}O_2CCH_3)_2(\eta^1\text{-}O_2CCH_3)(dppz)(CH_3OH)_3]^+$ (**2**; dppz = dipyrido[3,2-*a*:2′,3′-*c*]phenazine, Figure S1), is able to induce DNA strand breaks *in cellulo* at concentrations similar to that of cisplatin. A closely related compound with two N^N ligands, namely $[Rh_2(\mu\text{-}O_2CCH_3)_2(dppn)(dppz)(CH_3OH)_2]^{2+}$ (**3**; dppn = benzo[*i*]dipyrido[3,2-*a*:2,3-*c*]phenazine, Figure S1), was found to be active against the same cancer cell lines,[11] but it does not induce DNA damage at its cytotoxic concentration, supporting the contention that other mechanisms of action are switched on simply by changing the ligand environment around the dimetal unit.[11]

Recently, Che and co-workers[12] initiated a bioinformatics approach to identify the cellular targets of six dirhodium tetracarboxylate compounds, including the highly cytotoxic compound $Rh_2(\mu\text{-}O_2CCH_2CH_2CH_3)_4$. Results indicate that the biological signatures of these compounds are similar to that of the proteasome inhibitor MG-262, evidence that the ubiquitin–proteasome system (UPS) is a target of these compounds. Interestingly, it was also found that the highly cytotoxic dirhodium tetrapyrrolidinonato paddlewheel compound[12] does not inhibit UPS or cause DNA damage, supporting the hypothesis that different cellular targets can be reached by fine-tuning the nature of the equatorial ligands around the Rh_2^{4+} core.

In an effort to obtain further insight into the intracellular fate of dirhodium compounds and to identify key targets, we undertook the task of synthesizing and studying the subcellular localization of the fluorophore-labeled compound $[Rh_2(\mu\text{-}O_2CCH_3)_2(\eta^1\text{-}O_2CCH_3)(phenbodipy)(H_2O)_3][O_2CCH_3]$

Received: April 15, 2014
Published: May 22, 2014

dx.doi.org/10.1021/ja503774m | J. Am. Chem. Soc. 2014, 136, 7861–7864

(**1**; Figure 1) in human lung adenocarcinoma (A549) cells using laser scanning confocal fluorescence microscopy (Zeiss 510 Meta NLO). To our knowledge, compound **1** constitutes the first example of a M−M bonded compound tethered to a fluorescent organic probe.

To label the Rh_2^{4+} core, the polypyridyl ligand phenbodipy (Figure 1), which incorporates a green fluorescent bodipy moiety (4,4-difluoro-4-bora-3a,4a-diaza-*s*-indacene), was synthesized in three steps, as shown in Figure S2. It was obtained in good yields as a bright orange solid and characterized by NMR spectroscopy (Figure S4) and ESI-MS (m/z = 599.24 for $[phenbodipy+H]^+$). The dirhodium compound **1** was prepared by reacting $Rh_2(\mu\text{-}O_2CCH_3)_4$ with 1 equiv of phenbodipy in acetone for 24 h. The orange precipitate was suspended in methanol and stirred for another 24 h; the desired compound was obtained as an orange-brown solid upon precipitation with diethyl ether and was characterized by ESI-MS, NMR spectroscopy, and elemental analysis. The mass spectrum in methanol (Figure S5) contains three main peaks corresponding to $[M\text{-}O_2CCH_3\text{-}H]^+$ (m/z = 921), $[M]^+$ (m/z = 981), and $[M+CH_3OH]^+$ (m/z = 1013), where M = $[Rh_2(\mu\text{-}O_2CCH_3)_2(\eta^1\text{-}O_2CCH_3)(phenbodipy)]^+$.

The aliphatic region of the ^1H NMR spectrum of **1** is shown in Figure 2; the spectra of the related compounds $[Rh_2(\mu\text{-}O_2CCH_3)_2(\eta^1\text{-}O_2CCH_3)(N\text{^}N)(H_2O)_3][O_2CCH_3]$, where N^N = 1,10-phenanthroline (Rh_2phen) and 2,2′-bipyridine (Rh_2bpy), are also included (full spectra are included in Figures S6, S8, and S9). Compound **1** exhibits two singlet proton resonances at 1.02 and 1.06 ppm for the methyl group of $\eta^1\text{-}O_2CCH_3^-$ (Figure 2a), in contrast to one singlet for Rh_2phen (1.05 ppm, Figure 2b), Rh_2bpy (1.31 ppm, Figure 2c), and **2** (1.11 ppm)[11] for the same ligand. Since phenbodipy does not possess the C_{2v} symmetry of phen or bpy, compound **1** exists as a 1:1 mixture of geometric isomers that differ only by the relative position of the $\eta^1\text{-}O_2CCH_3$ ligand with respect to the triple bond of phenbodipy (Figure S7). The presence of four singlet resonances for the bridging ligands ($\mu\text{-}O_2CCH_3^-$) in **1** at 2.31, 2.32, 2.36, and 2.37 ppm (Figure 2a) further supports the existence of two geometric isomers.

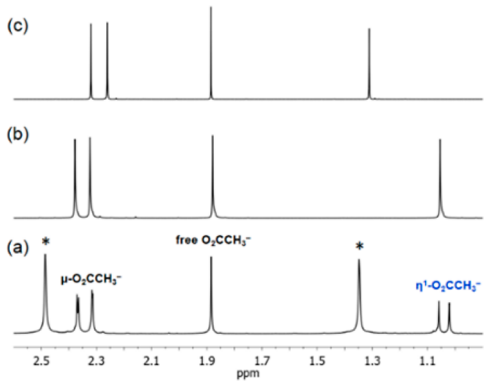

Figure 2. Portion of the ^1H NMR spectra of (a) **1**, (b) Rh_2phen, and (c) Rh_2bpy in CD_3OD, 500 MHz. The peaks marked with asterisks correspond to the $-CH_3$ groups of bound phenbodipy.

The electronic absorption spectra of phenbodipy and **1** are shown in Figure 3a. Both compounds exhibit an absorption maximum at 500 nm, with similar intensities ($\varepsilon = 6.7 \times 10^4$ and 5.9×10^4 M^{-1} cm^{-1}, respectively), that corresponds to a $^1\pi\pi^*$ ligand-centered (LC) transition involving the bodipy moiety.

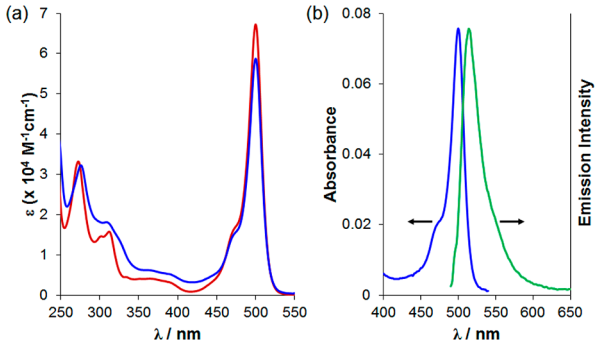

Figure 3. (a) Absorption spectra of phenbodipy (red) and **1** (blue) in MeOH. (b) Absorption (blue) and normalized emission (green, λ_{ex} = 496 nm) spectra of **1**.

Their absorption maxima in the UV region arise from superimposed $^1\pi\pi^*$ LC transitions of both bodipy and phenanthroline moieties. Compound **1** exhibits $Rh_2(\pi^*)\rightarrow phen(\pi^*)$ ^{1}MLCT transitions in the 400−450 nm range ($\varepsilon \approx 4 \times 10^3$ M^{-1} cm^{-1}), similar to the features reported for Rh_2phen (415 nm, $\varepsilon = 2.4 \times 10^3$ M^{-1} cm^{-1}) and Rh_2bpy (424 nm, $\varepsilon = 2.1 \times 10^3$ M^{-1} cm^{-1}).[13] Additionally, **1** exhibits a weak metal-centered $Rh_2(\pi^*)\rightarrow Rh_2(\sigma^*)$ transition at 625 nm (ε = 360 M^{-1} cm^{-1}, Figure S10), which is also observed for Rh_2phen (600 nm, 220 M^{-1} cm^{-1}), Rh_2bpy (598 nm, ε = 215 M^{-1} cm^{-1}), and related dirhodium compounds.[13−15] As expected, phenbodipy is fluorescent; the emission maximum is at 512 nm (λ_{ex} = 496 nm) and the fluorescence quantum yield (Φ_F) is 20% in aerated methanol solution, in agreement with similar systems.[16] The emission of phenbodipy in **1** is not completely quenched, with an emission maximum at 514 nm and Φ_F = 5% (Figure 3b) in the same solvent.

Tethering a fluorophore to non-luminescent metal drugs is a successful strategy for tracking their intracellular distribution using fluorescence microscopy.[17] In fact, this approach has been vital for understanding the mechanism of action of Pt(II) drugs. For example, imaging studies of fluorescein-labeled cisplatin analogues in U2-OS human osteosarcoma and ovarian carcinoma cells showed that these Pt drugs are sequestered into lysosomes, that they are accumulated into the nucleus and Golgi-derived vesicles, and also that they are colocalized with the copper efflux transporters ATP7A and ATP7B.[18−20] Platinum drugs formed by linking cisplatin units with anthraquinone[21] or with fluorescein-labeled diamine linkers[21] have been shown to accumulate in the nucleus of U2-OS cells. Although the emission from phenbodipy is partially quenched when the ligand is bound to the dimetal unit, we were nevertheless able to perform live cell imaging studies in cancer cells.

A549 cells were incubated with phenbodipy (1 μM) and **1** (1 μM) at 37 °C. As the images in Figure 4 attest, the cellular distributions of these compounds are different. The green fluorescence from phenbodipy indicates that the organic ligand is diffusely distributed throughout the cytoplasm, whereas **1** displays scattered distribution in the cytoplasm after 2 h of incubation. The fluorescence images did not change over a 24 h period (Figure S11). The distribution pattern of **1** is similar to that reported for Ru−polyarginine conjugates and could indicate that endocytosis is the mechanism of uptake.[23−25] The fact that the fluorescence emission distributions of phenbodipy and **1** are different suggests that the fluorophore is not detached from the dirhodium core in the time frame of

dx.doi.org/10.1021/ja503774m | J. Am. Chem. Soc. 2014, 136, 7861−7864

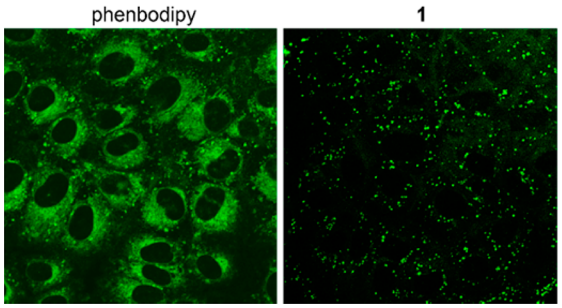

Figure 4. Confocal fluorescence images (143 μm × 143 μm) of 1 μM phenbodipy and 1 μM **1** after 2 h of incubation.

the experiments and that the cellular localization of **1** is dictated at least in part by the presence of the tethered dimetal moiety.[17] If detachment of the fluorophore were occurring, its emission intensity would increase considerably (since the Φ_F for phenbodipy is 4-fold greater than when it is bound to the Rh_2 fragment) and the cellular distribution would change, neither of which was observed.

To obtain further information on the subcellular localization of **1**, colocalization experiments with Lysotracker and Mitotracker (lysosome- and mitochondria-specific fluorescent trackers, respectively) were performed. These experiments were carried out at 10 and 100 μM concentrations since **1** is not cytotoxic in the 1−100 μM range. As shown in Figure 5a, there

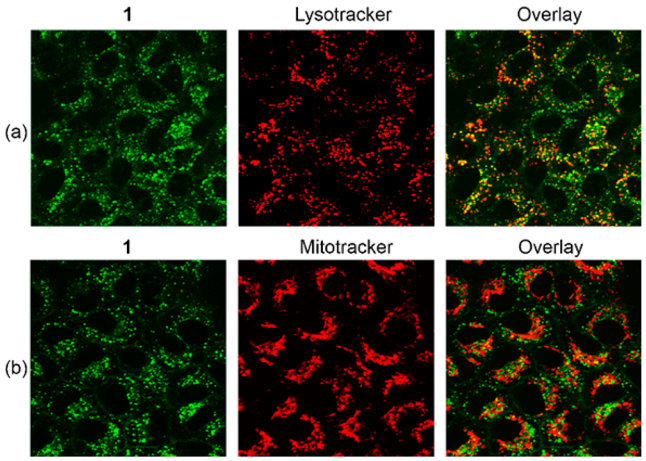

Figure 5. Confocal fluorescence images (105 μm × 105 μm) of (a) 10 μM **1** + Lysotracker and (b) 10 μM **1** + Mitotracker after 5 h of incubation.

is a good superposition pattern between the green fluorescence emission from **1** and the red fluorescence emission from Lysotracker after 5 h of incubation. The Mander's co-localization coefficient was 39.9 ± 4.0% (mean ± SD) at 10 μM **1**, indicating that there is ∼40% colocalization of the green fluorescence signal of **1** with the red fluorescence signal of Lysotracker. The coefficient is slightly larger (44.8 ± 4.4%) when the cells are incubated with 100 μM **1** for 5 h. After 24 h of incubation, the colocalization coefficients with Lysotracker decreased to 33.5 ± 6.0% and 32.3 ± 3.8% for 10 and 100 μM **1**, respectively. In the case of the localization of **1** in mitochodria (Figure 5b), the colocalization coefficients with Mitotracker were calculated to be 24.8 ± 2.3% and 31.0 ± 2.7% for 10 and 100 μM **1**, respectively, after 5 h of incubation, and remained essentially the same after 24 h of incubation at both concentrations (Figure S12). These results indicate that **1** localizes preferentially in lysosomes over mitochondria and that increasing the incubation time or concentration of **1** does not change its subcellular localization. Lysosome or mitochondria localization has also been reported for Ru compounds incorporating the dppz ligand[26] and free-base porphyrin−Ru(II) conjugates.[27]

Interestingly, green fluorescence emission from **1** was not observed in the nucleus of the cells in the 1−100 μM range of concentrations (Figure 6). Although the intracellular distribu-

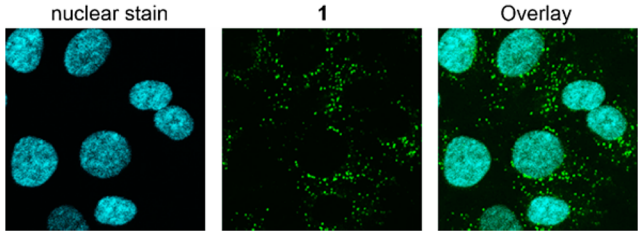

Figure 6. Confocal fluorescence images (75 μm × 75 μm) of Hoechst 33258 (nuclear stain) + 10 μM **1** after 24 h of incubation.

tion of **1** seems to be influenced mainly by the presence of the Rh_2^{4+} moiety, it is possible that the tethered bodipy fluorophore is influencing its biological properties and subcellular localization, which could explain the exclusion of **1** from the nucleus. The influence of a fluorophore on the localization of Ru(II) polypyridyl complexes conjugated to D-octaarginine peptides has been documented by Barton and co-workers,[23] where the intracellular localization of the Ru−peptide conjugate changed when fluorescein was covalently attached. The uptake of **1** was also measured after 24 h of incubation at 10, 50, and 100 μM concentrations. The mean emission intensity of **1** did not increase at concentrations greater than 50 μM (Figure S13), which could explain why the colocalization coefficients with Lysotracker (or Mitotracker) do not increase when the concentration was increased 10-fold.

To summarize, the first example of a M−M bonded compound incorporating an organic fluorophore has been synthesized. The present results with compound **1** indicate that dirhodium compounds can be tagged with fluorescent probes and that the intracellular localization is dictated at least in part by the tethered metal complex since the cellular distribution pattern of **1** differs from that of the free phenbodipy ligand. Compound **1** was found to target mainly lysosomes and mitochondria at concentrations in the 1−100 μM range, with a slight preference for the former organelle (∼1.4-fold). In contrast to the closely related compound **2** (see molecular structure in Figure S1), which targets the nucleus and induces DNA damage, compound **1** does not localize in the nuclei of A549 cells, evidence that supports the contention that various cellular organelles can be targeted by tuning the ligands of the dirhodium unit. In this vein, further studies are underway in our laboratories to modify the nature and lipophilicity of the fluorophore, to change its position relative to the dirhodium core (equatorial binding versus covalently attached to the bridging carboxylate ligands) in order to improve the uptake and cytotoxicity of this new type of fluorescent dirhodium compound. Ultimately, the aim is to gain deeper insight into the anticancer properties of this interesting class of M−M bonded compounds. Moreover, the current study provides an impetus for probing the biological properties of other

dx.doi.org/10.1021/ja503774m | J. Am. Chem. Soc. 2014, 136, 7861−7864

multicenter inorganic complexes, since the same strategy can be used to label diruthenium[28] and dirhenium[29] anticancer compounds. It is worth pointing out that the realization that Rh−Rh bonded compounds can be successfully tagged with light-harvesting units such as bodipy will positively impact other research areas, such as the use of dirhodium compounds as photocatalysts,[30−32] since attaching a moiety with a high molar absorptivity to the dimetal core is expected to improve the efficiency of such catalytic systems.

■ ASSOCIATED CONTENT

Ⓢ Supporting Information

Experimental procedures, NMR and electronic absorption spectra, and microscopy images. This material is available free of charge via the Internet at http://pubs.acs.org.

■ AUTHOR INFORMATION

Corresponding Authors

rmouneimne@cvm.tamu.edu
dunbar@mail.chem.tamu.edu

Notes

The authors declare no competing financial interest.

■ ACKNOWLEDGMENTS

K.R.D. gratefully acknowledges the National Science Foundation (NSF 02-465401-00001) for support of this work. Confocal microscopy studies were performed in the Texas A&M University College of Veterinary Medicine & Biomedical Sciences Image Analysis Laboratory, supported by NIH-NCRR (1S10RR22532-01).

■ REFERENCES

(1) Chifotides, H. T.; Dunbar, K. R. *Acc. Chem. Res.* **2005**, *38*, 146−156.
(2) Rosenberg, B.; VanCamp, L.; Trosko, J. E. *Nature* **1969**, *222*, 385−386.
(3) Erck, A.; Rainen, L.; Whileyman, J.; Chang, I. M.; Kimball, A. P.; Bear, J. *Proc. Soc. Exp. Biol. Med.* **1974**, *145*, 1278−1283.
(4) Howard, R. A.; Sherwood, E.; Erck, A.; Kimball, A. P.; Bear, J. L. *J. Med. Chem.* **1977**, *20*, 943−946.
(5) Fimiani, V.; Ainis, T.; Cavallaro, A.; Piraino, P. *J. Chemother.* **1990**, *2*, 319−326.
(6) Espósito, B. P.; Zyngier, S. B.; de Souza, A. R.; Najjar, R. *Met. Based Drugs* **1997**, *4*, 333−338.
(7) Aguirre, J. D.; Chifotides, H. T.; Angeles-Boza, A. M.; Chouai, A.; Turro, C.; Dunbar, K. R. *Inorg. Chem.* **2009**, *48*, 4435−4444.
(8) Angeles-Boza, A. M.; Chifotides, H. T.; Aguirre, J. D.; Chouai, A.; Fu, P. K. L.; Dunbar, K. R.; Turro, C. *J. Med. Chem.* **2006**, *49*, 6841−6847.
(9) Sherman, S. E.; Lippard, S. J. *Chem. Rev.* **1987**, *87*, 1153−1181.
(10) Aguirre, J. D.; Angeles-Boza, A. M.; Chouai, A.; Pellois, J.-P.; Turro, C.; Dunbar, K. R. *J. Am. Chem. Soc.* **2009**, *131*, 11353−11360.
(11) Aguirre, J. D.; Angeles-Boza, A. M.; Chouai, A.; Turro, C.; Pellois, J.-P.; Dunbar, K. R. *Dalton Trans.* **2009**, 10806−10812.
(12) Siu, F.-M.; Lin, I. W.-S.; Yan, K.; Lok, C.-N.; Low, K.-H.; Leung, T. Y.-C.; Lam, T.-L.; Che, C.-M. *Chem. Sci.* **2012**, *3*, 1785−1793.
(13) Crawford, C. A.; Matonic, J. H.; Streib, W. E.; Huffman, J. C.; Dunbar, K. R.; Christou, G. *Inorg. Chem.* **1993**, *32*, 3125−3133.
(14) Crawford, C. A.; Matonic, J. H.; Huffman, J. C.; Folting, K.; Dunbar, K. R.; Christou, G. *Inorg. Chem.* **1997**, *36*, 2361−2371.
(15) Joyce, L. E.; Aguirre, J. D.; Angeles-Boza, A. M.; Chouai, A.; Fu, P. K. L.; Dunbar, K. R.; Turro, C. *Inorg. Chem.* **2010**, *49*, 5371−5376.
(16) Cui, A.; Peng, X.; Fan, J.; Chen, X.; Wu, Y.; Guo, B. *Photochem. Photobiol. A: Chem.* **2007**, *186*, 85−92.
(17) Klein, A. V.; Hambley, T. W. *Chem. Rev.* **2009**, *109*, 4911−4920.
(18) Molenaar, C.; Teuben, J. M.; Heetebrij, R. J.; Tanke, H. J.; Reedijk, J. *J. Biol. Inorg. Chem.* **2000**, *5*, 655−665.
(19) Katano, K.; Safaei, R.; Samimi, G.; Holzer, A.; Tomioka, M.; Goodman, M.; Howell, S. B. *Clin. Cancer. Res.* **2004**, *10*, 4578−4588.
(20) Safaei, R.; Katano, K.; Larson, B. J.; Samimi, G.; Holzer, A. K.; Naerdemann, W.; Tomioka, M.; Goodman, M.; Howell, S. B. *Clin. Cancer. Res.* **2005**, *11*, 756−767.
(21) Kalayda, G.; Jansen, B. J.; Wielaard, P.; Tanke, H.; Reedijk, J. *J. Biol. Inorg. Chem.* **2005**, *10*, 305−315.
(22) Kalayda, G. V.; Zhang, G.; Abraham, T.; Tanke, H. J.; Reedijk, J. *J. Med. Chem.* **2005**, *48*, 5191−5202.
(23) Puckett, C. A.; Barton, J. K. *J. Am. Chem. Soc.* **2009**, *131*, 8738−8739.
(24) Puckett, C. A.; Barton, J. K. *Bioorg. Med. Chem.* **2010**, *18*, 3564−3569.
(25) Cosgrave, L.; Devocelle, M.; Forster, R. J.; Keyes, T. E. *Chem. Commun.* **2010**, *46*, 103−105.
(26) Pierroz, V.; Joshi, T.; Leonidova, A.; Mari, C.; Schur, J.; Ott, I.; Spiccia, L.; Ferrari, S.; Gasser, G. *J. Am. Chem. Soc.* **2012**, *134*, 20376−20387.
(27) Zhang, J.-X.; Zhou, J.-W.; Chan, C.-F.; Lau, T. C.-K.; Kwong, D. W. J.; Tam, H.-L.; Mak, N.-K.; Wong, K.-L.; Wong, W.-K. *Bioconjugate Chem.* **2012**, *23*, 1623−1638.
(28) Silva, D. d. O. *Anticancer Agents Med. Chem.* **2010**, *10*, 312−323.
(29) Shtemenko, N. I.; Chifotides, H. T.; Domasevitch, K. V.; Golichenko, A. A.; Babiy, S. A.; Li, Z.; Paramonova, K. V.; Shtemenko, A. V.; Dunbar, K. R. *J. Inorg. Biochem.* **2013**, *129*, 127−134.
(30) Xie, J.; Li, C.; Zhou, Q.; Wang, W.; Hou, Y.; Zhang, B.; Wang, X. *Inorg. Chem.* **2012**, *51*, 6376−6384.
(31) Heyduk, A. F.; Nocera, D. G. *Science* **2001**, *293*, 1639−1641.
(32) Powers, D. C.; Chambers, M. B.; Teets, T. S.; Elgrishi, N.; Anderson, B. L.; Nocera, D. G. *Chem. Sci.* **2013**, *4*, 2880−2885.